International Journal of Science and Research (IJSR)
ISSN: 2319-7064
SJIF (2020): 7.803

Design, Analysis, and Testing of Shape Memory Alloy based Robotic Morphing Wing

Dhanesh Pamnani[1], Ganesh Jeughale[2]

[1, 2]K. J. Somaiya College of Engineering

Abstract: ***This research paper focuses on design, analysis, and testing of a smart robotic wing, which can morph its shape between two airfoils depending on the environmental conditions. Shape Memory Alloy (SMA)(Ni-Ti) is used to obtain the unique morphing of the robotic wing. It also discusses in detail the design flow, CAD, components, and CFD analysis and results for DRS in FSAE style racecar. Further, the paper presents the testing of the Ni-Ti alloy to obtain the morphing temperature and the challenges in training the wing. Finally, the future scope of this technology and the parameters to consider are also discussed.***

Keywords: Shape Memory Alloy, smart robots, active aerodynamics, morphing wings, Drag Reduction System

1. Introduction

Robotics allows us to improve efficiency in every walk of life by performing tasks more efficiently. Robotics can be divided into multiple subdomains including mechatronics, perception, planning, control systems, and soft robotics. One of the growing areas of research is soft robotics as it finds its applications in the medical, aerospace, defense, and commercial industries. Soft robotics encompasses any system which can change its shape as per the requirement of the user. Shape memory alloys enable the development of smart soft robots. These can be seen in medical devices, humanoid systems, as well as various other systems. SMAs are also actively being used in the aerospace sector. Combining these two, an application of SMA can be in soft wings which have the ability to morph its shape based on the environmental conditions and user inputs.

This application will help design smarter UAVs which have multi-dimensional abilities, for example, a maneuverable UAV can also act as a glider if its airfoil is changed. Another application can be in a VTOL UAV where the SMA can give the robot ability to hover and fly. Similarly, the application can be in performance vehicles like F1 and FSAE. The Drag Reduction System which is used are usually very heavy and bulky. Using SMA robotic morphing wing will allow changing the airfoil structure and hence the drag force without the weight penalty. Further, having a morphing wing will allow the wing to be mounted firmly and have a very linear morphing instead of sudden change of angle of attack.

Thus, the SMA can find various applications as a smart robotic wing. The further sections give a detailed CAD design, CFD, FEA analysis, and testing training of the SMA robotic wing. The CFD results, turbulence modeling, laboratory experiments results, challenges and future scope are also discussed of this application of robotic wing.

2. Literature Review

2.1 SMA properties

SMA are materials that have the ability to recover a large elastic deformation under thermomechanical loading. They display two distinct phases - martensite (low temperature phase) and austenite (high temperature phase). Under the application of sufficient thermal or mechanical stress, the reorientation of twinned martensite into detwinned martensite can take place. Due to variation in orientation and variations in local stress concentrations, this micromechanical normalizing leads to a smoother material response, as different grains experience transformation at different points in the thermomechanical loading path. One-way shape memory effect is when the metal can be bent or stretched and will hold those shapes when it is in the cold or martensite state. Upon heating, the shape changes to its original. Materials having shape memory effect both during heating and cooling are said to possess two-way shape memory effect. This is possible because the SMA remembers its old shape by leaving some small crystalline reminders of the original low-temperature condition even during the high temperature phases.

2.2 CFD turbulence model

The designs are analyzed using computational fluid dynamics (CFD) for the drag and downforce estimations. It is an external flow simulation over the front wing, where the flow would be turbulent; hence the first step would be finding the Reynolds number of the flow.

At low Reynolds numbers, flows tend to be dominated by laminar (sheet-like) flow, while at high Reynolds numbers turbulence results from differences in the fluid's speed and direction, which may sometimes intersect or even move counter to the overall direction of the flow. It is given by

$$\mathrm{Re} = \frac{\rho u L}{\mu} = \frac{u L}{\nu}$$

Calculating the Reynolds number for density= 1.225, v=16m/s and length = effective chord length the flow will be laminar in the frontal half and become turbulent towards the trailing edge. The analysis in such cases is done by solving the Navier Stokes equations which are differential equations of pressure and velocity. In the case of a compressible Newtonian fluid, these yields

$$\underbrace{\rho\left(\frac{\partial \mathbf{u}}{\partial t} + \mathbf{u}\cdot\nabla\mathbf{u}\right)}_{1} = \underbrace{-\nabla p}_{2} + \underbrace{\nabla\cdot\left(\mu(\nabla\mathbf{u} + (\nabla\mathbf{u})^{T}) - \frac{2}{3}\mu(\nabla\cdot\mathbf{u})\mathbf{I}\right)}_{3} + \underbrace{\mathbf{F}}_{4}$$

where **u** is the fluid velocity, ***p*** is the fluid pressure, ***ρ*** is the fluid density, and ***μ*** is the fluid dynamic viscosity. The different terms correspond to the inertial forces (1), pressure forces (2), viscous forces (3), and the external forces applied

to the fluid (4).

In engineering applications where the Reynolds number is very high, the inertial forces (1) are much larger than the viscous forces (3). Such turbulent flow problems are transient in nature; a mesh that is fine enough to resolve the size of the smallest eddies in the flow needs to be used.

Instead, we can use a Reynolds-Averaged Navier-Stokes (RANS). The turbulent viscosity, μT, is evaluated using turbulence models. The most common one is the k-w SST turbulence model. The use of a k-ω formulation in the inner parts of the boundary layer makes the model directly usable all the way down to the wall through the viscous sublayer, hence the SST k-ω model can be used as a Low-Re turbulence model without any extra damping functions. The SST formulation also switches to a k-ε behavior in the free-stream and thereby the model is not too sensitive to the inlet free-stream turbulence properties. Two equation models for the turbulence kinetic energy, k, and turbulence specific dissipation rate, ω. Aims to overcome the deficiencies of the standard k-omega model wrt dependency on the free stream values of k and omega. Able to capture flow separation

Thus, this turbulent model was chosen for the CFD study. Simscale software was selected for the analysis as it is based on Openfoam and is a cloud-based software which allows for parallel computing on 16-32 core processors.

3. Design Flow

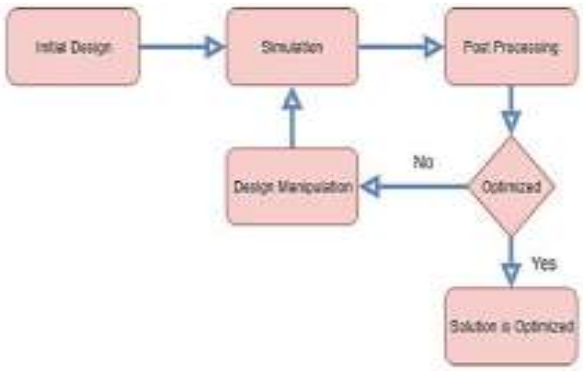

Figure 1: Design Flow

4. CAD of the Morphing Robot

The CAD of the front wing of an FSAE style racecar has been presented here. The initial and final design of the SMA auxiliary wing is also shown in the side view so that the different airfoils can be understood. The detailed design of the SMA robotic wing has also been shown. SMA wires are used to connect the leading edge of the wing to the trailing edge. The number of wires is also calculated based on the heat required to morph the wires the resistance of the wires and the voltage and current supplied by the battery.

The side wall of the wing is also presented here. Using Shape Memory Alloy wires for the side wall allows to have morphing characteristics in the side wall which can help redirect the air around the front tires.

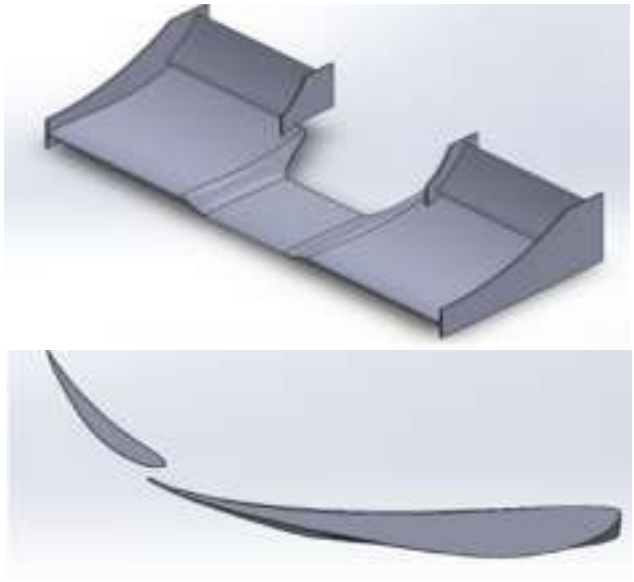

Figure 2: Initial Front Wing CAD

Figure 3: SMA wing CAD

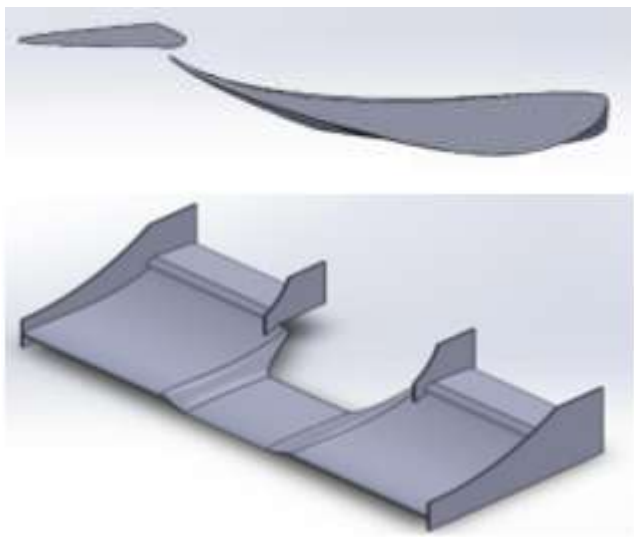

Figure 4: Final Front Wing CAD

Figure 5: Endplate CAD with SMA wires

5. CFD and FEA analysis

The working fluid for the study is air. The density of air is taken as 1.225kg/m^3 and the kinematic viscosity is 0.000015295 m^2/s. The initial conditions are as follows

- pressure = 0 Pa
- Velocity = 0 m/s
- k = 0.24 m^2/s^2
- w = 44.7 1/s

The boundary conditions for the flow were inlet velocity, outlet pressure, moving wall velocity, no slip condition on the wing and slip condition on the walls. The slip condition allows the solver to think of the walls as air and the wall isn't solved for shear stresses and hence drag is not calculated at the walls. The floor however is given a moving wall velocity function because it induces ground effect on the wing as discussed in the previous chapter.

The ground moves relative to the wing. In the computational model the wing is at rest and the air column and the ground are moving. Hence the inlet velocity has a velocity of 16m/s in the negative z direction. The moving wall velocity also has 16m/s in the negative z direction. The wing is given a boundary condition of no slip thus ensuring viscous drag and shear force is calculated at the wing.

Results for High Downforce initial SMA configuration
The value of Downforce is 223.2N and of Drag is 53.67N. Hence, lift coefficient of 2.91, drag coefficient as 0.701. The efficiency was obtained to be 4.151.

The pressure contour for this iteration is as shown

Figure 6: Pressure contour High Downforce

The ground effect can be seen as suction is strongest at the closest point. The high pressure above the wing pushes it down creating downforce. The low pressure behind the wing is responsible for wake and drag. It also causes flow separation as shown in the following velocity contour and flow streamline.

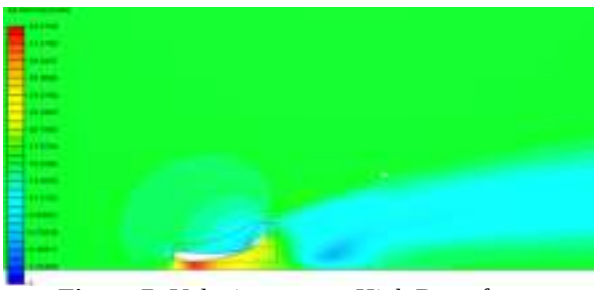

Figure 7: Velocity contour High Downforce

The low velocity region is the region of flow separation and contributes to drag. This region is called the wake region and is mainly caused because of the vortices.

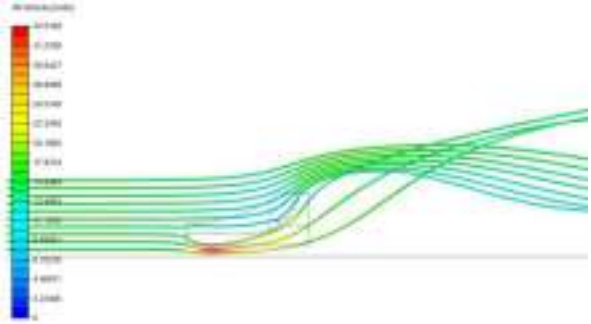

Figure 8: Velocity flow lines High Downforce

Results for Low Drag Morphed Wing Shape The low drag iteration was similarly computed, and the pressure and velocity contours and the streamlines were obtained. The drag value was 11.12N and downforce was 95.23N. The lift coefficient is 1.244 and of drag is 0.1452. The efficiency calculated is 8.5674.

The pressure contour is as follows

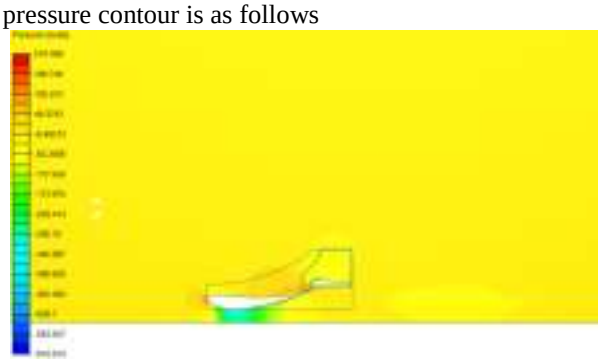

Figure 9: Pressure contour morphed low drag

The velocity contour is shown in the figure. The wake is clearly diminished. There is no flow separation which in turn reduces vortices and size of the wake region and hence drag. This also results in greater efficiency of the wing

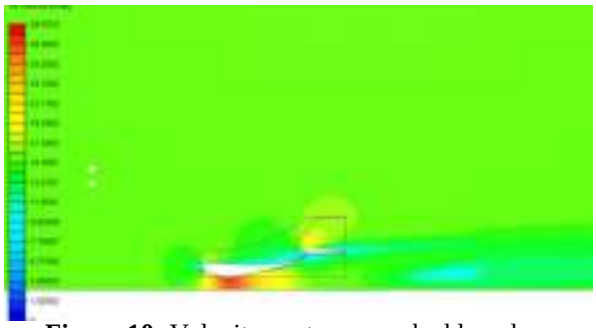

Figure 10: Velocity contour morphed low drag

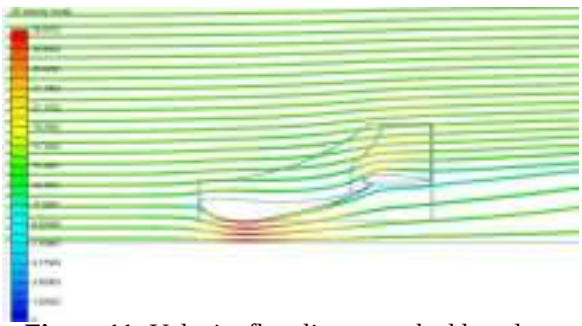

Figure 11: Velocity flow lines morphed low drag

Thus, the values obtained are tabulated below.

Table 1: Results table

Parameter	High Downforce	Low drag	Remarks
Downforce	223.2N	95.23N	57% decrease
Drag	53.67N	11.12 N	79% decrease
CL	2.91	1.244	
CD	0.701	0.145	
Efficiency	4.151	8..5674	106% increase
Wake Region Size	76cm	8cm	89.47% decrease

Finite Element Analysis

FEA was done on the leading edge of the airfoil. The leading edge was made of PLA by additive manufacturing methods. A FEA was done for ensuring that the structure can take the loads.

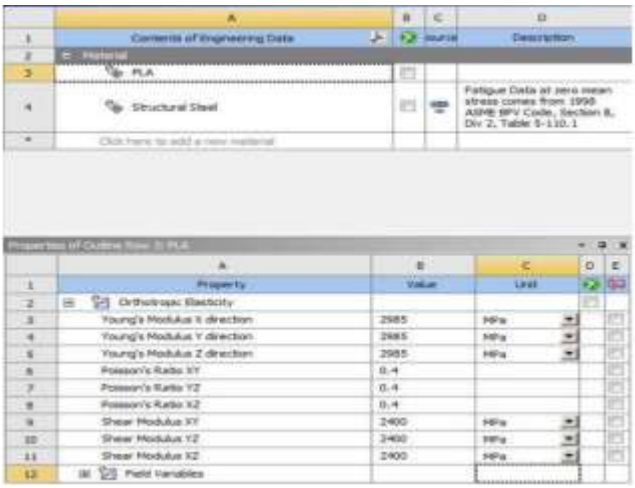

Figure 12: Material properties

The material was tested for equivalent stress and strain. The strain was found to be 0.01137 MPA and strain $3.25*10^{-6}$. Thus, the structure is safe for the drag loads.

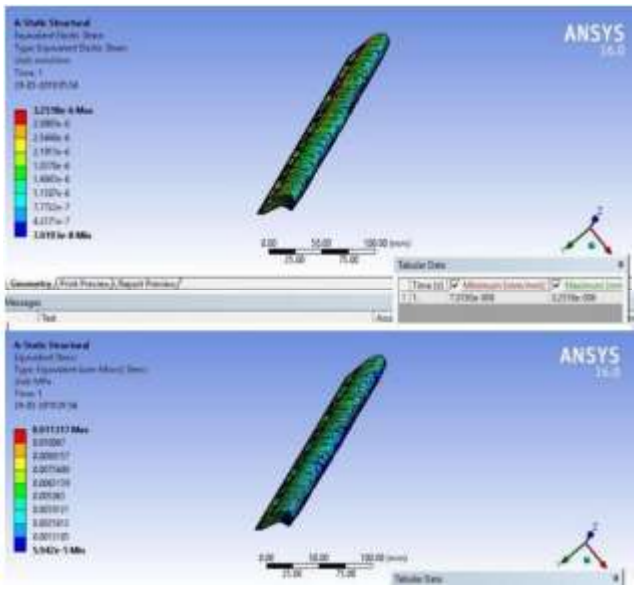

Figure 13: FEA results

5.1 Experimental testing and prototyping

It is already known that there are 4 transformation temperature with SMA, mainly martensite start, martensite finish, austenite start, and austenite finish. Our purpose of interest is only with austenite temperatures, so we carried out experiment just to determine them. To get approximate estimation of As and Af we carried out a small experiment in chemistry lab. Following were the apparatus used, Flask, Thermometer, Bunsen burner with tripod, SMA wire of 0.5 mm diameter, 200 ml water

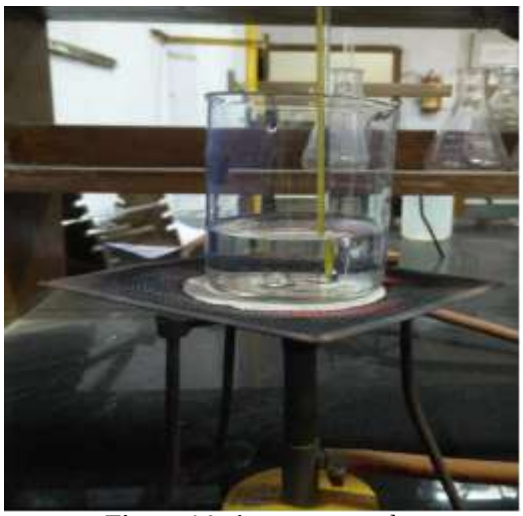

Figure 14: Apparatus results

At first to get the idea range of transformation temperature five beakers containing water at different temperature ranging from 40C to 80C were taken. 5 spring shape wire of length 12 cm each were made and when the respective temperature was reached wire was immersed in beaker i.e once 40 C was reached 1st coil was dipped and effect was noted, when beaker 2 reached 50C 2nd coil was dipped similarly other wires were tested.

Room temperature = 32C, Initial water temperature = 31C

Table 2: Water-time-SMA morphing table

S.No.	Water Temp	Time (Sec)	Effect wire
1	40	45	No change
2	50	96	No change
3	60	140	Partially uncoiled
4	70	210	Completely uncoiled
5	80	255	Completely uncoiled

The changes are recorded in the following pictures,

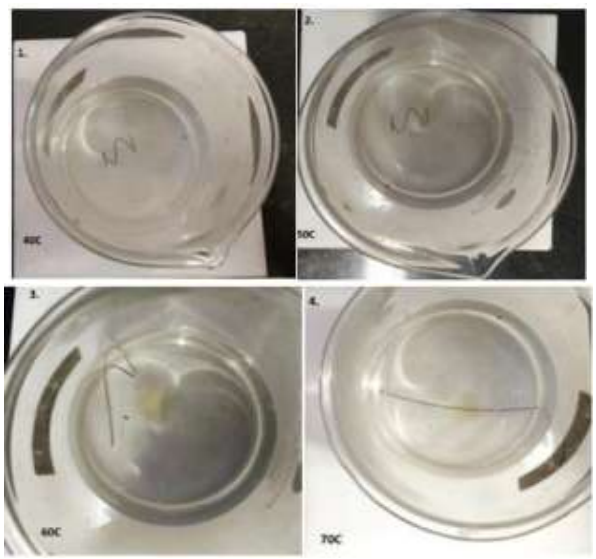

Figure 15: Changes in SMA morphing

Further, testing was done with continuous heating and the following results were obtained,

Table 3: Continuous heating Water-time-SMA morphing

S.No.	Water Temp	Effect on wire
1	40	Coiled
2	45	Coiled
3	45-54	Coiled
4	55	Uncoiling starts
5	58	Partially uncoiled & Further Uncoiling
6	66	Completely uncoiled
7	66-70	No change in shape

Next, the SMA wires were trained by both one way and two-way memory effect; this allowed shifting between two shapes

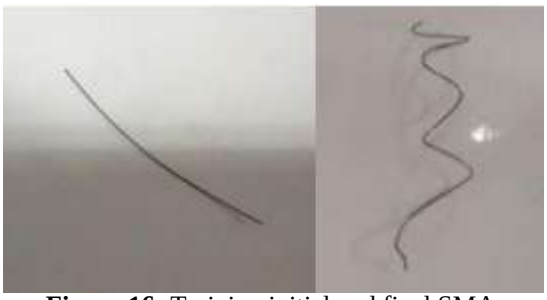

Figure 16: Training initial and final SMA

6. Conclusion

This paper thus presents the potential SMA application area in robotic morphing wing. The wing is made of various SMA wires which are tested for their morphing temperatures and trained to have a cold and hot shape. Application of this smart wing for active aerodynamics in a glider or the wing of a racecar is discussed. The CAD of the front wing DRS of a FSAE style racecar is also presented. Further the CFD and FEA analysis show that this morphing wing technique can lead to better performance with minimum weight penalty. Alloy chosen for the concept is NITINOL due to its superior characteristics like higher strength, better response time, low current requirement, and longer life. Detailed design of the robotic wing and CFD simulations of the FSAE car to verify the drag reduction have been discussed. There is a rise in the efficiency by 106% while a drop in downforce by 57% and drag by 79%.

Thus, the morphed wing not only reduces the drag but also increases the aerodynamic efficiency. It is light in weight than any other DRS system currently used. It is also more dynamic and gives much more control to the operator. It is low power consuming and houses its own power source. SMA based morphing of wings is the most efficient and effective way of actively controlling the aerodynamics of the racecar. Further, the SMA wires are tested to obtain the morphing temperatures, through lab experiments, and the wires are then trained and electronically tested to check the change between the two airfoil shapes. Thus, the design, analysis and testing of a robotic wing is obtained which can be used for active aerodynamics in DRS or UAVs

7. Future Scope

Further attempts should be made to induce two-way shape memory effect using various other training techniques. Focus should be made to reduce battery size and power requirement which could be achieved if heat dissipates through wire is reduced. Refinement of model and other parameters if needed and analysis for same. The use of SMA as a DRS for FSAE style racecar works well in theory however there are complications when it comes to manufacturing that needs to be worked on. A method to heat and cool the wires instantaneously needs to be thought about. The structure needs to be made more rigid for it to be mounted on the vehicle, carbon fiber can be used for this. Electrical work needs to be more concise

Reference

[1] Paulo Silva Loboa,b, Joao Almeida a, Lu´ıs Guerreiroa, Shape memory alloys behaviour: A review, Elsevier,Procedia Engineering 114 (2015).
[2] D J Hartl and D C Lagoudas∗, Aerospace applications of shape memory alloys, Department of Aerospace Engineering, Texas A&M University, College Station, Texas, USA.
[3] Mohammad Mahdi Kheirikhah, Samaneh Rabiee, and Mohammad Ehsan Edalat, A Review of Shape Memory Alloy Actuators in Robotics, Islamic Azad
[4] University, Faculty of Industrial & Mechanical Engineering,Nokhbegan Boulevard, Qazvin, Iran
[5] G. Airoldi, T. Ranucci, G. Riva, mechanical and electrical properties of a niti shape memory alloy, [5] Katz,j.(n.d), Aerodynamics of race car.
[6] Milliken, W., & Milliken, D. (n.d), race car vehicle dynamics.
[7] Dhanesh Pamnani, Ganesh Jeughale, "Smart Robotic Morphing Wing for Active Aerodynamics using Shape Memory Alloy", International Journal of Science and Research (IJSR)
[8] Merkel, J. (2013). Development of multi-element active aerodynamics.
[9] O. M. A. Taha, M. B. Bahrom, O. Y. Taha, and M. S. Aris, experimental study on two way shape memory effect training procedure for nitiol shape memory alloy, ARPN Journal of Engineering and Applied Sciences (2015).
[10] H Y uo, and E W Abel, A comparison of methods for the training of NiTi two-way shape memory alloy,smart materials and structure.
[11] L.G. Machado and M.A. Savi, Medical applications of shape memory alloys, Brazilian Journal of Medical and Biological Research (2003).
[12] Jensen,K.(n.d). aerodynamic undertray design for formula SAE.
[13] Bansal, R.K (n.d), Fluid Mechanics and Hydraulics machines.
[14] UIUC.(n.d), Airfoil Database.
[15] Milliken, W.,& Milliken, D.(n.d), Aerodynamics of Formula Sae:A numerical, wind Tunnel and On track study
[16] Lisa Case,Zachary Kreiner, John Redmond, and Brian Trease, Shape Memory Alloy Shape Training Tutorial,Smart Materials and Structures(2004).